

# Molecular beam epitaxy growth of InAs and $\text{In}_{0.8}\text{Ga}_{0.2}\text{As}$ channel materials on GaAs substrate for metal oxide semiconductor field effect transistor applications

Ning Li,<sup>a)</sup> Eric S. Harmon, and David B. Salzman  
*Lightspin Technologies, Inc., P.O. Box 30198, Bethesda, Maryland 20824-0198*

Dmitri N. Zakharov, Jong-Hyeok Jeon, Eric Stach, and Jerry M. Woodall  
*Department of Electrical Engineering, Purdue University, West Lafayette, Indiana 47907*

X. W. Wang, T. P. Ma, and Fred Walker  
*Yale University, 15 Prospect St., New Haven, Connecticut 06520*

(Received 26 October 2007; accepted 24 March 2008; published 30 May 2008)

InAs and high indium concentration InGaAs have very high electron mobilities and saturation velocities. Using them as the metal oxide semiconductor field effect transistor (MOSFET) channel materials is a very promising way to keep improving the integrated circuit chip performance beyond Moore's law. One major obstacle is the growth of these high mobility channel materials on lattice-mismatched substrates. In this work, we studied the molecular beam epitaxy growth of InAs,  $\text{In}_{0.8}\text{Al}_{0.2}\text{As}$ , and  $\text{In}_{0.8}\text{Ga}_{0.2}\text{As}$  on lattice-mismatched GaAs substrate using a thin indium-rich InAs wetting layer. Reflection high energy electron diffraction and atomic force microscopy were used to optimize the growth conditions. A surface roughness of  $\sim 0.5$  nm rms was obtained for InAs layers. A new MOSFET structure with  $\text{In}_{0.8}\text{Ga}_{0.2}\text{As}$  channel and  $\text{In}_{0.8}\text{Al}_{0.2}\text{As}$  buffer layer was also demonstrated. High mobility depletion mode MOSFET characteristics were demonstrated.

© 2008 American Vacuum Society. [DOI: 10.1116/1.2912086]

The rapid growth of the IC industry is based on the continuous scaling of silicon complementary metal oxide semiconductor devices to smaller sizes. However, further scaling becomes more and more problematic as the channel length approaches 22 nm. The major problems include high power density, large variability, severe parasitics, etc. The use of high mobility III–V channel materials has emerged as a promising solution and is currently under intensive investigation.<sup>1</sup> Among all III–V semiconductor materials, InAs and high indium content InGaAs exhibit superior combinations of high electron mobility and high saturation velocity. For pure InAs, the electron mobility and saturation velocity are  $\sim 33\,000\text{ cm}^2\text{ V}^{-1}\text{ s}^{-1}$  and  $\sim 8 \times 10^7\text{ cm/s}$ , respectively.<sup>2</sup> These values are both a factor of four higher than GaAs-based channels that have recently been studied for logic applications.<sup>3</sup>

However, the lack of a high surface quality in heteroepitaxially grown InAs films has been a major obstacle to the development of their metal oxide semiconductor field effect transistor (MOSFET) devices where even nanometer-scale roughness can degrade transport. The problem is due to the large lattice mismatch between InAs and common III–V substrates such as GaAs and InP. We approach the heteroepitaxy of InAs on GaAs with the view of integrating these materials with silicon through a GaAs/Ge buffer.<sup>4</sup> In this work, we used reflection high energy electron diffraction (RHEED), atomic force microscopy (AFM), and transmission electron microscopy (TEM) to fully characterize the growth conditions for flat InAs films on (001) GaAs substrates. Besides

pure InAs, we also grew high indium content InGaAs using similar method. These InGaAs materials retain similar mobility as InAs while having a larger band gap. Comparing with the high leakage current associated with the narrow bandgap bulk InAs,<sup>5</sup> InGaAs channels could have lower leakage. We designed, fabricated and characterized a heteroepitaxial MOSFET structure that incorporates an  $\text{In}_{0.8}\text{Ga}_{0.2}\text{As}$  channel on an  $\text{In}_{0.8}\text{Al}_{0.2}\text{As}$  buffer layer grown on a GaAs substrate.

As a starting point for our material growth, we used an approach developed by Chen *et al.*<sup>6</sup> and Chang *et al.*<sup>7</sup> for the growth of InAs on GaP via a wetting layer. The wetting layer is grown under As-poor conditions so that a continuous, smooth, In-rich film forms in the first nanometer. This In-rich film reacts with the underlying GaAs buffer layer, resulting in a smooth compositional grading of the interface reminiscent of a liquid phase epitaxial reaction.<sup>7</sup> To determine the As-poor conditions required for the wetting layer, we measure the surface phase diagram using RHEED in Fig. 1. At low As flux, the InAs surface has an In-rich  $4 \times 2$  reconstruction; while at high As flux, the InAs surface has an As-rich  $2 \times 4$  reconstruction. Optimal growth as determined by AFM was found for a 5-nm-thick InAs wetting layer deposited using the In-rich condition at  $485\text{ }^\circ\text{C}$  substrate temperature and a beam equivalent As pressure of  $3 \times 10^{-6}$  Torr, as indicated with a star in Fig. 1. Following the deposition of the wetting layer, the As flux was increased to achieve As-rich conditions for the rest of the growth to avoid the formation of metallic In droplets. Figure 2 shows the RHEED pattern during the InAs wetting layer growth. The RHEED pattern turned from stripes to spots after the first nanometer of

<sup>a)</sup>Electronic mail: ningli@ee.ucla.edu

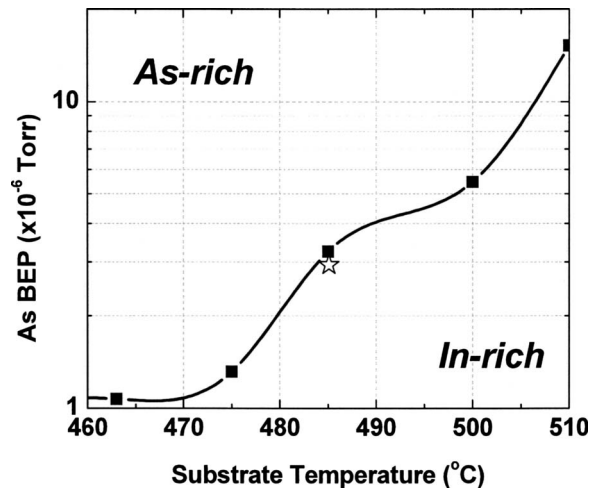


FIG. 1. Measured surface phase diagram of InAs using RHEED. The solid squares are the measured As beam equivalent pressure at which the InAs surface reconstruction changed from As rich ( $2\times 4$ ) to In rich ( $4\times 2$ ). The star indicates the growth conditions for the InAs wetting layer used to optimize the surface morphology.

growth, and then changed back to streaky pattern as the wetting layer thickness reached 4 nm.

As consequence of this wetting layer, a  $1\text{-}\mu\text{m}$ -thick film of epitaxially grown InAs has a surface roughness of  $\sim 0.5\text{ nm rms}$  in a  $5\times 5\ \mu\text{m}^2$  area (see Fig. 3). Previously, compositionally graded buffer layers<sup>8-11</sup> have been used to improve the epitaxial InAs film quality on GaAs. However, the grown film usually has a surface roughness on the order of several nanometers.<sup>9,11</sup> Thick GaSb or AlSb buffer layers<sup>12</sup> have also been used to further improve smoothness of the InAs. In this case, the surface roughness can reach  $\sim 1\text{ nm}$  or below but the implementation is limited by the availability of the Sb source. Our surface roughness result obtained by growing InAs directly on GaAs substrate is among the best reported for metamorphic growth of InAs. Importantly, no cross-hatch pattern was observed on the wafer surface. Figure 4 is a microscope image of the grown InAs wafer surface. It shows the surface morphology on a much larger scale than the AFM image. The oval defect density is on the order of  $\sim 3000\text{ cm}^{-2}$ . There is no evidence of the formation of indium droplets. Figure 5 shows the TEM

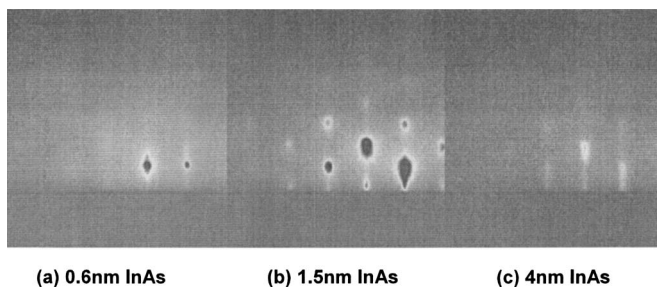


FIG. 2. RHEED pattern during the InAs wetting layer growth at the film thickness of (a) 0.6 nm, (b) 1.5 nm, and (c) 4 nm. This sequence of images indicates a progression from two dimensional (2D) wetting to three dimensional nucleation to 2D growth within just a few nanometers.

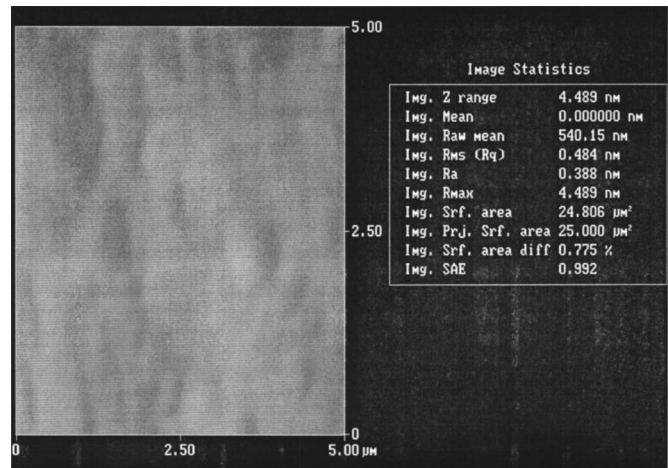


FIG. 3. AFM image of the surface of the epitaxially grown InAs using the wetting layer.

cross-sectional images and diffraction patterns. Stacking faults are observed in Fig. 5(a). The diffraction pattern showed that the film is single crystalline. The abrupt lattice constant change across the InAs/GaAs interface is clearly seen in Fig. 5(c). The strain is partially relaxed at the inter-

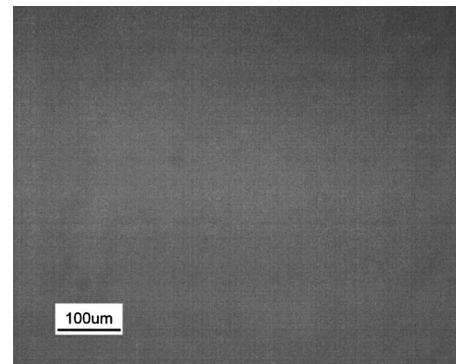


FIG. 4. Optical microscope image of the epitaxially grown InAs.

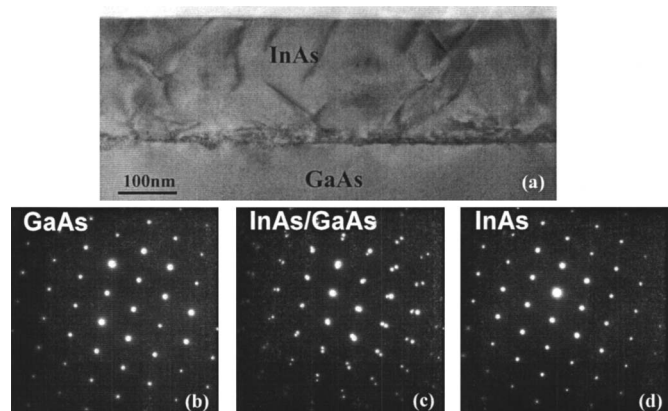


FIG. 5. (a) TEM cross-sectional images and (b) diffraction pattern in GaAs substrate at (c) InAs/GaAs interface, and (d) inside InAs epilayer. The images show how the wetting layer confines the defects to the first few nanometers over which the RHEED transition takes place in Fig. 2. The diffraction patterns show a relaxed film at the interface.

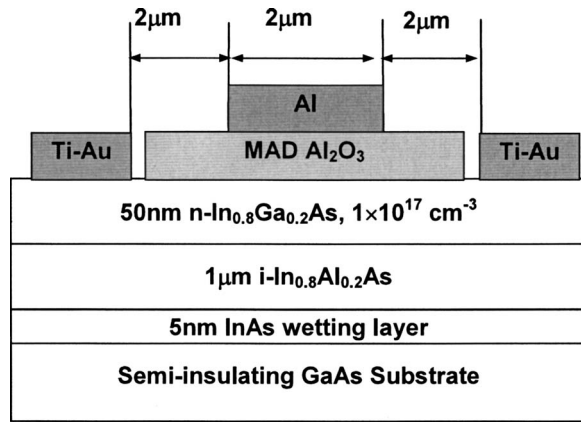


FIG. 6. Designed and fabricated GaAs/ $\text{In}_{0.8}\text{Ga}_{0.2}\text{As}$ /MAD- $\text{Al}_2\text{O}_3$  MOSFET structure.

face by misfit dislocations. However, local strain is still present in the film volume, as can be seen in Fig. 5(a).

A MOSFET structure is designed to characterize the epitaxial material quality and optimize device performance at room temperature (Fig. 6). In order to reduce off current, we used  $\text{In}_{0.8}\text{Ga}_{0.2}\text{As}$  instead of pure InAs as the channel material. A 1- $\mu\text{m}$ -thick  $\text{In}_{0.8}\text{Al}_{0.2}\text{As}$  buffer layer was first grown

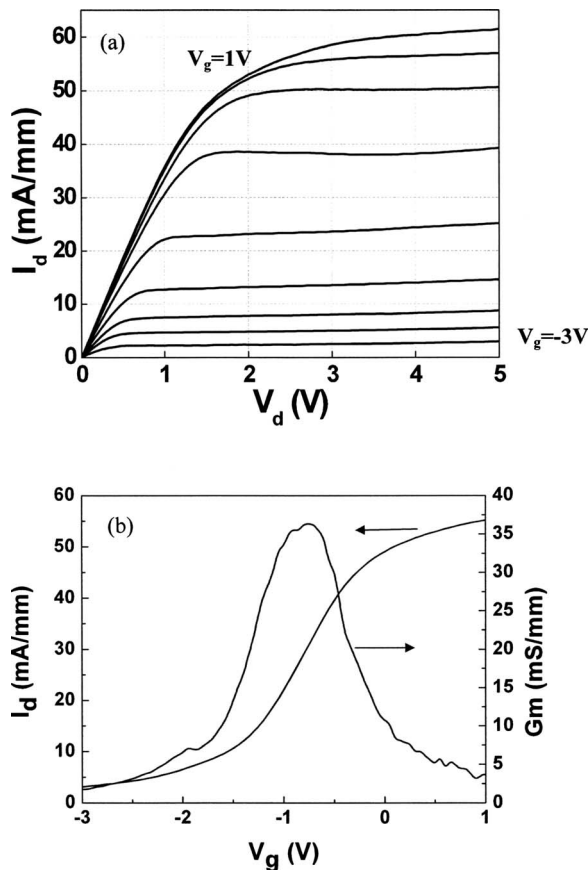


FIG. 7. Measured GaAs/ $\text{In}_{0.8}\text{Ga}_{0.2}\text{As}$ /MAD- $\text{Al}_2\text{O}_3$  MOSFET  $I$ - $V$  characteristics including (a)  $I_d$  (drain current)- $V_d$  (drain voltage) curves from  $V_g$  (gate voltage) = -3 - 1 V with 0.5 V step from the bottom to the top, and (b)  $I_d$ - $V_g$  and  $G_m$  (transconductance)- $V_g$  curves at  $V_d = 4$  V.

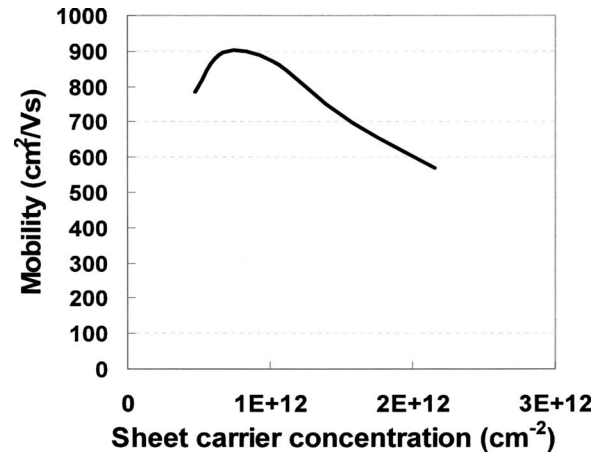


FIG. 8. Extracted GaAs/ $\text{In}_{0.8}\text{Ga}_{0.2}\text{As}$ /MAD- $\text{Al}_2\text{O}_3$  MOSFET channel mobility vs carrier concentration.

on top of the InAs wetting layer, followed by the deposition of a 50-nm-thick channel layer of  $n\text{-In}_{0.8}\text{Ga}_{0.2}\text{As}$  ( $5 \times 10^{16} \text{ cm}^{-3}$ ). The Hall mobility measured on this MBE grown InGaAs sample is  $\sim 6000 \text{ cm}^2/\text{V s}$  at room temperature. AFM analysis indicates a surface roughness of 3.5 nm rms for the sample with 1  $\mu\text{m}$   $\text{In}_{0.8}\text{Al}_{0.2}\text{As}$  grown on top of the InAs wetting layer. The reason for the degraded surface roughness is believed to be a low mobility of the Al atom at the low growth temperature.

On top of the  $\text{In}_{0.8}\text{Ga}_{0.2}\text{As}$  channel material, a layer of  $\text{Al}_2\text{O}_3$  was deposited with molecular-atom-deposition<sup>13</sup> (MAD) method as the gate dielectric. Ti-Au was used as the source/drain contact metal. Al was used as the gate metal. Figure 7 shows the  $I_d$ - $V_d$  characteristics of this metamorphic  $\text{In}_{0.8}\text{Ga}_{0.2}\text{As}$  device. From the capacitance-voltage ( $CV$ ) measurement, the equivalent oxide thickness was  $\sim 21$  nm. Despite the thick gate dielectric, good channel current and transconductance ( $\sim 40 \text{ mS/mm}$ ) were obtained. Figure 8 shows the extracted channel mobility versus the sheet carrier concentration, after correcting for source and drain series resistance but without correcting for interface states. The extracted mobility number is comparable to the value reported recently in other high mobility InGaAs buried channel devices,<sup>14</sup> where a AlInAs heterojunction barrier is used to protect the channel region from the deposited gate dielectric.

In conclusion, we studied the MBE growth of InAs,  $\text{In}_{0.8}\text{Al}_{0.2}\text{As}$ , and  $\text{In}_{0.8}\text{Ga}_{0.2}\text{As}$  on GaAs substrate. RHEED and AFM were used to optimize the growth conditions. Improved surface morphology was observed when we carefully controlled the nucleation conditions at each heteroepitaxial transition. We also demonstrated MOSFETs with  $\text{In}_{0.8}\text{Ga}_{0.2}\text{As}$  channel grown on GaAs. By scaling the channel length and dielectric thickness, significant improvements in drive current and transconductance can be expected.

## ACKNOWLEDGMENTS

Fred Walker would like to acknowledge primary support from the National Science Foundation under Contract No. MRSEC DMR 0520495.

- <sup>1</sup>R. Chau *et al.*, *IEEE Trans. Nanotechnol.* **4**, 153 (2005).
- <sup>2</sup>K. Brennan and K. Hess, *Solid-State Electron.* **27**, 347 (1984).
- <sup>3</sup>Y. Xuan, H. Lin, P. D. Ye, and G. D. Wilk, *Appl. Phys. Lett.* **88**, 263518 (2006).
- <sup>4</sup>J. A. Carlin, S. A. Ringe, E. A. Fitzgerald, and M. Bulsara, *Prog. Photovoltaics* **8**(3), 323 (2000).
- <sup>5</sup>N. Li, E. Harmon, J. Hyland, D. Salzman, T. P. Ma, Y. Xuan, and P. D. Ye, *Appl. Phys. Lett.* **92**, 143507 (2008).
- <sup>6</sup>A. Chen, A. Yulius, and J. M. Woodall, *Appl. Phys. Lett.* **85**, 3447 (2004).
- <sup>7</sup>J. C. P. Chang, T. P. Chang, and J. M. Woodall, *Appl. Phys. Lett.* **69**, 981 (1996).
- <sup>8</sup>T. Nee, R. Lin, L. Hsieh, and L. Chang, *J. Vac. Sci. Technol. A* **20**, 1128 (2002).
- <sup>9</sup>C. Karlsson, N. Rorsman, S. Wang, and M. Persson, *IEEE International Symposium on Compound Semiconductors*, 1997 (unpublished), pp. 483–486.
- <sup>10</sup>S. E. Hooper, D. I. Westwood, D. A. Woolf, S. S. Heghoyan, and R. H. Williams, *Semicond. Sci. Technol.* **8**, 1069 (1993).
- <sup>11</sup>A. A. Khandekar, G. Suranarayanan, S. E. Babcock, and T. F. Kuech, *J. Cryst. Growth* **292**, 40 (2006).
- <sup>12</sup>B. R. Bennett, Brad P. Tinkham, J. Brad Boos, M. D. Lange, and Roger Tsai, *J. Vac. Sci. Technol. B* **22**, 688 (2004).
- <sup>13</sup>T. P. Ma, *IEEE Trans. Electron Devices* **45**, 680 (1998).
- <sup>14</sup>Y. Sun, E. W. Kiewra, J. P. De Souza, S. J. Koester, K. E. Fogel, and D. K. Sadana, *Device Research Conference*, June 2007 (unpublished), pp. 209–210.